

Non-local detection of resistance fluctuations of an open quantum dot

A. I. Lerescu, E. J. Koop, C. H. van der Wal, and B. J. van Wees
*Physics of Nanodevices Group, Zernike Institute for Advanced Materials,
 University of Groningen, Nijenborgh 4, 9747 AG Groningen, The Netherlands*

J. H. Bardarson

Instituut-Lorentz, Universiteit Leiden, P.O. Box 9506, 2300 RA Leiden, The Netherlands

(Dated: February 6, 2020)

We investigate quantum fluctuations in the non-local resistance of an open quantum dot which is connected to four reservoirs via quantum point contacts. In this four-terminal quantum dot the voltage path can be separated from the current path. We measured non-local resistance fluctuations of several hundreds of Ohms, which have been characterized as a function of bias voltage, gate voltage and perpendicular magnetic field. The amplitude of the resistance fluctuations is strongly reduced when the coupling between the voltage probes and the dot is enhanced. Along with experimental results, we present a theoretical analysis based on the Landauer-Büttiker formalism. While the theory predicts non-local resistance fluctuations of considerably larger amplitude than what has been observed, agreement with theory is very good if an additional dephasing mechanism is assumed.

PACS numbers: 73.23.-b, 73.63.Kv, 73.40.-c

I. INTRODUCTION

When a conducting solid-state system is smaller than the phase coherence length of the electrons, its electrical conductance is significantly influenced by quantum interference. For diffusive thin films this results in phenomena known as universal conductance fluctuations and weak localization^{1,2,3,4}. Similar conductance fluctuations and localization phenomena are observed in micron-scale ballistic quantum dots, since these behave in practice as chaotic cavities due to small shape irregularities in the potential that defines the dot. These conductance fluctuations have been extensively studied for two-terminal quantum dots^{5,6,7,8}, *i.e.* systems with only a source and a drain contact. However, for quantum dots this two-terminal conductance is often influenced by Coulomb blockade and weak localization effects, which complicate an analysis when one aims at studying other effects.

We present here a study of fluctuations in electron transport in a *four*-terminal ballistic quantum dot. The dot is coupled to four reservoirs via quantum point contacts (QPC). In such a system, the voltage path (with probes at voltage V_+ and V_-) can be separated from the path that is used for applying a bias current I (see Fig. 1). Consequently, one can measure so-called *non-local*^{9,10,11,12} voltage signals that are purely due to quantum fluctuations of the chemical potential¹³ inside the dot, and for which a naive classical analysis predicts a signal very close to zero. For linear response, this is expressed as a non-local resistance $R_{nl} = (V_+ - V_-)/I$ (this non-local resistance will fluctuate around a value that is very close to zero Ohm, and is therefore studied in terms of resistance rather than conductance). Increasing the number of open channels in the voltage probes will result in enhanced dephasing for the electrons. With a four-terminal system, one can study this directly since it results in a reduction of the amplitude

of the non-local resistance fluctuations. Notably, such a reduction of the fluctuation amplitude does not occur upon increasing the number of open channels in a two-terminal system¹⁴. Furthermore, such a four-terminal systems could be used for studying signals that are due to spin. In a strong magnetic field QPCs can be operated as spin-selective injectors or voltage probes¹⁵. This can be used to generate and detect an imbalance in the chemical potential for spin-up and spin-down electrons¹⁶, similar to non-local spin-valve effects observed in metallic nanodevices¹⁷. Also here, a four-terminal dot is an interesting alternative to work on spin physics in dots with two-terminal devices^{18,19,20}. However, if such a system is smaller than the electron phase coherence length, the non-local signals with information about spin will also show fluctuations that result from interference of electron trajectories²¹.

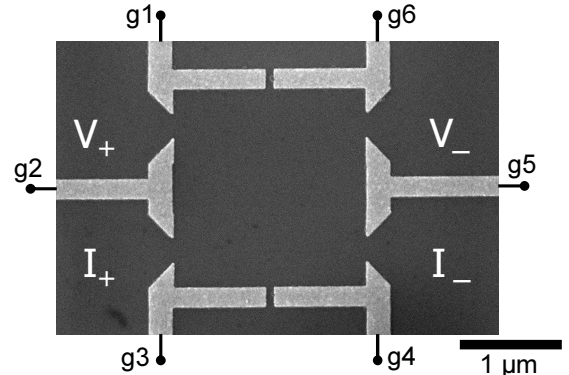


FIG. 1: Electron microscope image of the device studied in this article. The position of the reservoirs used for current biasing (I_+ and I_-) and voltage probes (V_+ and V_-) is indicated, as well as the numbering of the gates labeled $g1$ - $g6$. Unless stated otherwise, all results presented in this article were obtained in this non-local configuration.

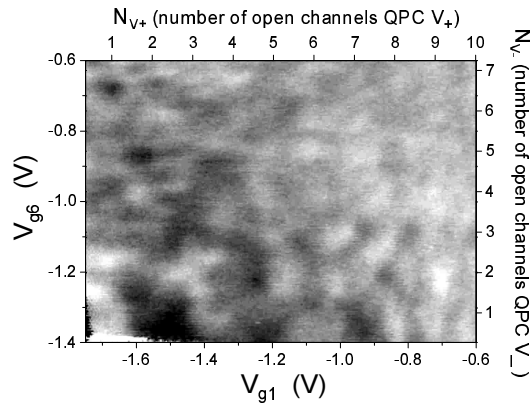


FIG. 2: Gray scale plot of the non-local resistance R_{nl} as a function the voltages applied to gates $g1$ and $g6$. The axes also show the corresponding number of open channels for the V_+ and V_- probes. The gray scale shows R_{nl} at a scale from -500Ω (black) to 500Ω (white). The value of R_{nl} fluctuates around zero Ohm, with a typical amplitude that decreases when the number of open channels in the V_+ and V_- probes increases. The QPCs formed by gates $g2$ and $g3$, as well as $g4$ and $g5$ (defining the current path) had a fixed conductance of $2e^2/h$ each. Data taken in zero magnetic field at 130 mK.

In this article, we focus on our first experiments with such a four-terminal quantum dot. We aimed at characterizing the non-local resistance fluctuations, and studying the influence of the voltage probes on the typical amplitude of these fluctuations. As a comparison with our experimental results we present a numerical simulation of the non-local resistance, based on the Landauer-Büttiker formalism^{9,22} and the kicked rotator^{23,24}.

The outline of the paper is as follows: Section II presents the experimental realization. In section III, we present measurements of the non-local resistance as a function of bias voltage, gate voltage, and magnetic field, and confirm that the observed fluctuations in the non-local resistance are the four-terminal equivalent of universal conductance fluctuations in two-terminal systems. In section IV, we analyze how the typical amplitude of the measured non-local resistance fluctuations depends on the number of open channels in the voltage probes. Section V presents our theoretical analysis with a comparison to the experimental results, before ending with conclusions.

II. EXPERIMENTAL REALIZATION

Our device was fabricated using a GaAs/ $\text{Al}_x\text{Ga}_{1-x}\text{As}$ heterostructure containing a two dimensional electron gas (2DEG) 75 nm below the surface, purchased from Sumitomo Electric Co. At 4.2 K, the mobility was $\mu = 86 \text{ m}^2/\text{Vs}$ and the electron density was $n_s = 2.4 \cdot 10^{15} \text{ m}^{-2}$. The dot was designed with an area of $2 \times 2 \mu\text{m}^2$. Figure 1 shows and electron microscope image of the device. Six depletion gates were deposited

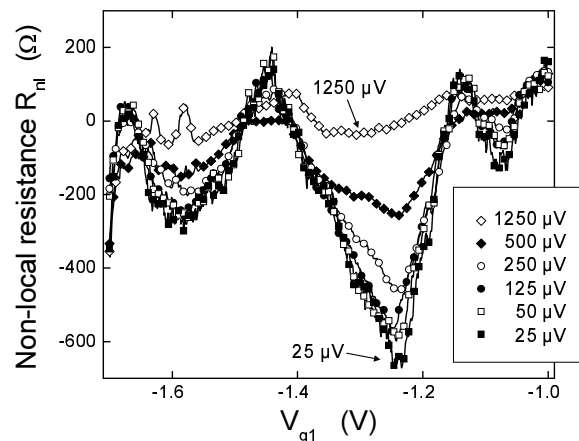


FIG. 3: The non-local resistance R_{nl} as a function of the voltage V_{g1} applied to gate $g1$, taken for different amplitudes of the bias current I in the lock-in detection scheme (from 1 nA up to 50 nA). The legend shows the corresponding values for the voltage drop across the quantum dot along the current path, obtained as $V_{bias} \approx I \times \frac{2}{2e^2/h}$. The curves show a reduction of the amplitude of the non-local resistance fluctuations with increasing V_{bias} . The conductance of the QPC formed by $g5$ and $g6$ (defining the V_- probe) is set at $2e^2/h$. For further experimental parameters see Fig. 2.

on the surface (15 nm of Au with a Ti sticking layer) and were used for defining the dot in the 2DEG. Thus, the dot could also be coupled to the four reservoirs via QPCs in a controllable manner. All four QPCs showed clear quantized conductance steps^{25,26} in measurements where only the corresponding pair of gates were depleting the 2DEG. Note that throughout this article we use that a QPC with a conductance of $2e^2/h$ is defined as having one open channel (denoted as $N = 1$), *i.e.* we neglect spin when counting channels. The four reservoirs were connected to macroscopic leads via Ohmic contacts, which were realized by annealing a thin Au/Ge/Ni layer that was deposited on the surface.

All the measurements were performed with the sample at a temperature of 130 mK. We used a current bias I with standard ac lock-in techniques at 13 Hz. Unless stated otherwise, we used $I = 1 \text{ nA}$. The non-local resistance R_{nl} was then recorded as the zero-bias differential resistance dV/dI , with V defined as $V \equiv V_+ - V_-$. We used a floating voltmeter to measure V , thus being insensitive to the voltage across the dot along the current path, and thereby insensitive to Coulomb blockade and weak localization effects. On the current path, only the I_- reservoir was connected to the grounded shielding of our setup, and all gate voltages were applied with respect to this ground.

A magnetic field could be applied, with an angle of 7° with respect to the 2DEG plane (determined from standard Hall measurements and electron focusing effects, discussed below). The perpendicular component of this field was used for studying the dependence of the

non-local resistance on perpendicular magnetic field. The component of the magnetic field parallel with the 2DEG plane was oriented perpendicular to the current path. While this parallel field was about ten times stronger than the perpendicular field, the orbital effects associated with this parallel field are negligibly small, and it can be disregarded for all of the experimental results presented here (and weak enough to not significantly reduce the amplitude of resistance fluctuations^{27,28,29}).

III. NON-LOCAL RESISTANCE FLUCTUATIONS

Figure 2 shows the non-local resistance R_{nl} as a function of the voltage applied to gate $g1$ and gate $g6$. The other four gate voltages were kept constant during this measurement, with the QPCs in the current path at a conductance of $2e^2/h$ each (one open channel, $N = 1$). The range of gate voltage for $g1$ and $g6$ used here corresponds to opening the voltage-probe QPCs from nearly pinched off ($N = 0$) up to about $N = 8$ open channels. As a function of these gate voltages, the non-local resistance shows a random pattern of fluctuations around zero Ohm, with maximums and minimums up to about $\pm 500 \Omega$. Notably, the change in gate voltage needed to change R_{nl} significantly (one fluctuation), is very similar to the change in gate voltage needed for increasing the number of open channels in a QPC by one. This corresponds to changing the shape of the potential that forms the dot by a distance of about half a Fermi wavelength, which is consistent with the length scale needed for significantly changing a random interference pattern of electron trajectories. These non-local resistance fluctuations as a function of the gate voltage on $g1$ and $g6$ were highly reproducible, and indeed a so-called fingerprint of the sample. The identical measurement repeated after 4 days (during which we performed strong magnetic field sweeps and a temperature cycle up to 4.2 K) showed nominally the same fluctuation pattern as in Fig. 2.

In Fig. 3 we present results of studying the dependence of the amplitude of the non-local resistance fluctuations on the amplitude of the applied bias current I . The figure shows measurements of R_{nl} as a function of the gate voltage V_{g1} . The results show several fluctuations that are reproducible, but decreasing in amplitude upon increasing the amplitude of the bias current. In this experiment, the conductance of the other three QPCs was fixed at $2e^2/h$. The amplitude of the fluctuations reduces when the measurement averages over contributions of electrons in uncorrelated orbitals, that is, averaging over electrons that differ in energy by more than the Thouless energy^{3,4}. When the current bias is increased, the corresponding voltage bias V_{bias} increases as well (see labels in the Fig. 3), and this is used to experimentally estimate the Thouless energy E_{Th} for our system. The amplitude of the fluctuations starts to decrease significantly around $V_{bias} \approx 125 \mu V$. This is close

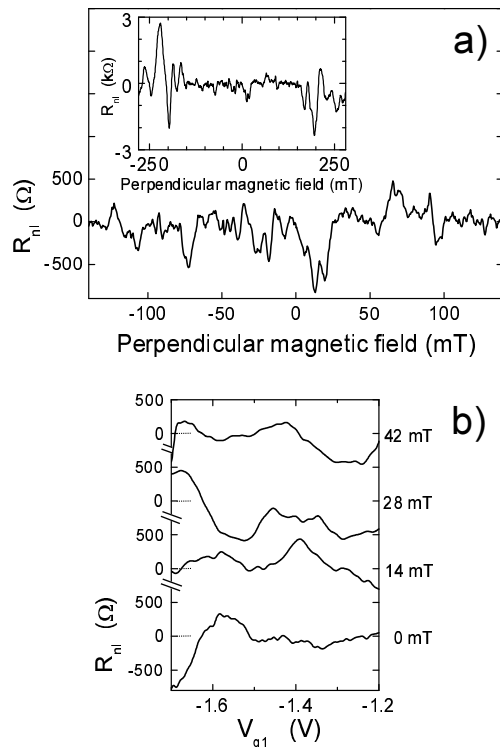


FIG. 4: a) The non-local resistance R_{nl} as a function of magnetic field. The magnetic field is given on the scale of the perpendicular component of the total applied field. For this measurement all four QPCs are defined to have a conductance of $2e^2/h$. The inset presents the same data for a wider range of the magnetic field, showing the onset of electron focusing effects for perpendicular fields larger than ± 140 mT. The curves in b) show the non-local resistance as a function of the voltage applied to gate $g1$ at different values of the perpendicular magnetic field. The conductance of the QPC formed by $g5$ and $g6$ (defining the V_- probe) is kept at $2e^2/h$. For further experimental parameters see Fig. 2.

to a theoretical estimate^{30,31} for $E_{Th} = \frac{\hbar v_F}{L} \approx 80 \mu eV$, where v_F the Fermi velocity and L the effective width of the dot.

We now turn to measurements of the non-local resistance as a function of perpendicular magnetic field, presented in Fig. 4a. Here the conductance of all four QPCs was fixed at $2e^2/h$. The trace of R_{nl} shows random fluctuations of similar amplitude as observed in the gate voltage dependence. From the limited amount of data in this trace (we did not use data from fields in excess of ± 140 mT, see below), the magnetic field scale for significantly changing the value of R_{nl} (the correlation field ΔB_c) is estimated to be around 10 mT. For obtaining a more precise estimate, we studied fluctuations in R_{nl} as a function of gate voltage V_{g1} , for different values of the perpendicular field (Fig. 4b). This data confirms that changing the perpendicular magnetic field gives access to completely different patterns of random fluctuations in R_{nl} . The changes appear to be significant

only after increasing the applied perpendicular field by 14 mT or more. This is in good agreement with the theoretical value $\Delta B_c = C(\frac{h}{e})\frac{1}{L^2}$, from theory for universal conductance fluctuations³. For the constant $C = 1$, the formula simply expresses the magnetic field needed for adding one flux quantum h/e through the dot, and gives a value of $\Delta B_c \approx 1.2$ mT for the effective area of our dot. The discrepancy between the measured value and this estimate for $C = 1$, can be explained by the fact that ΔB_c is enhanced by a factor of ~ 2 due to flux cancellation effects for electrons that move ballistically between the edges of the dot^{2,32}. Further, ΔB_c is enhanced by a factor $\sqrt[4]{n_{dot}} \approx 9$ (where $n_{dot} \approx 8000$ the number of electrons in the dot), because electrons have a finite dwell time in the dot, and the relevant area before escape of typical trajectories is therefore smaller than the dot³⁰. The measured value for ΔB_c is in agreement with the width of a weak-localization peak around zero magnetic field³, observed in the two-terminal resistance (breaking the time-reversal symmetry).

The inset of Fig. 4a) shows the appearance of much higher peaks in R_{nl} (up to 3 k Ω) for perpendicular magnetic fields stronger than ± 140 mT. We could confirm that these peaks are due to electron focusing and skipping orbit effects. With only the three gates g_1 , g_2 and g_3 depleting the 2DEG, our device is identical to devices used for electron focusing experiments by Van Houten *et al.*³³, and we observe very similar focusing peaks as in this work at only one polarity of the magnetic field. With the dot formed, these effects cause peaks in R_{nl} at both polarities of the magnetic field. The onset of these effects at ± 140 mT agrees with a focusing radius of about 1 μm .

IV. INFLUENCE OF VOLTAGE PROBES

The presence of additional voltage probes on a quantum dot system will act as source of dephasing for the electrons in the dot, and this effect should increase when the coupling between the dot and the probe reservoirs is enhanced. Earlier work recognized that non-local voltage probes on a mesoscopic system are a source of dephasing^{34,35}, and in theoretical work an additional voltage probe is often used to model a source of dephasing^{36,37}. This can be directly studied with our system. The amplitude of the non-local resistance fluctuations (which result from electron phase coherence) should decrease when the voltage probes are tuned to carry more open channels. To study this effect we used data sets of the type presented in Fig. 2. We concentrate on the case where the time-reversal symmetry is broken ($\beta = 2$) by applying weak magnetic fields, since this allows us to get statistics from a larger set of data.

For a data set as in Fig. 2, the total number of open channels in the voltage probes ($N_{V+} + N_{V-}$) is lowest in the bottom left corner of the graph, and highest in the top right corner. Inspection of R_{nl} in Fig. 2 confirms that the typical amplitude of the fluctuations de-

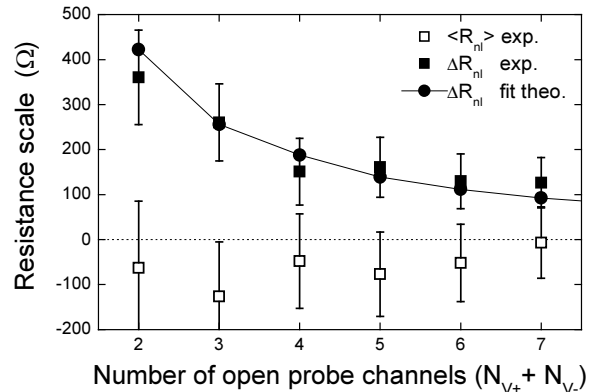


FIG. 5: Dependence of the mean $\langle R_{nl} \rangle$ and rms standard deviation ΔR_{nl} of fluctuations in the measured non-local resistance R_{nl} , as a function of the total number open of channels in the voltage probes $N_{V+} + N_{V-}$ (squared dots). The statistics are from sets of data as in Fig. 2, but with time-reversal symmetry broken by weak magnetic fields ($\beta = 2$). The round dots with solid line present a fit of the theoretical model that describes the values of ΔR_{nl} (see text for details).

creases when the voltage probes get more open channels. For a more quantitative analysis of this observation, we determined the mean $\langle R_{nl} \rangle$ and root-mean-square (rms) standard deviation ΔR_{nl} of the non-local resistance for traces recorded at a fixed number of channels in the voltage probes. This can be obtained by following R_{nl} along lines with constant $N_{V+} + N_{V-}$. The theory in the next section shows that, on such a line, ΔR_{nl} should also show a weak dependence on $N_{V+} - N_{V-}$. However, we do not have sufficient data to study this, and simply average along lines with constant $N_{V+} + N_{V-}$. The results of this analysis are presented in Fig. 5. The large error bars for $\langle R_{nl} \rangle$ and ΔR_{nl} in Fig. 5 are due to the fact that we could only record a finite number of independent data sets with fluctuations in R_{nl} (see Ref. 38 for further details).

The results in Fig. 5 confirm that $\langle R_{nl} \rangle$ is very close to zero, for all values of $N_{V+} + N_{V-}$. More interestingly, ΔR_{nl} smoothly decreases as a function $N_{V+} + N_{V-}$, demonstrating directly the dephasing influence of the voltage probes for the electrons in the quantum dot. The typical fluctuation amplitude approaches zero when the dot becomes fully open (very strong coupling to a reservoir). For a quantitative evaluation of this observation, we will first present a theoretical model in the next Section.

V. THEORETICAL ANALYSIS

For our theoretical modeling we consider a ballistic chaotic cavity connected to four reservoirs through quantum point contacts. A net current I flows between two of the contacts (from I_+ to I_-), while there is no net

current flowing into two contacts used as voltage probes (contacts V_+ and V_-). We use the Landauer-Büttiker

formalism to derive the relations between the current I and the voltages of the four contacts²¹,

$$I = \frac{1}{2} \left(\frac{2e^2}{h} \right) [(N_1 - T_{11}) + (N_2 - T_{22}) + T_{12} + T_{21}] \frac{V_{bias}}{2} + (T_{23} - T_{13})V_3 + (T_{24} - T_{14})V_4, \quad (1a)$$

$$V_3 = \frac{V_{bias}}{2} \frac{(N_4 - T_{44})(T_{31} - T_{32}) + T_{34}(T_{41} - T_{42})}{(N_3 - T_{33})(N_4 - T_{44}) - T_{34}T_{43}}, \quad (1b)$$

$$V_4 = \frac{V_{bias}}{2} \frac{(N_3 - T_{33})(T_{41} - T_{42}) + T_{43}(T_{31} - T_{32})}{(N_3 - T_{33})(N_4 - T_{44}) - T_{34}T_{43}}, \quad (1c)$$

where we used (for concise labeling) notation according to

$$\begin{aligned} I_+ &\leftrightarrow 1, \\ I_- &\leftrightarrow 2, \\ V_+ &\leftrightarrow 3, \\ V_- &\leftrightarrow 4. \end{aligned}$$

Here the T_{ij} are the transmission probabilities from contact i to j , while the N_i are the number of open channels in contact i . The voltages V_i are all defined with respect to a ground³⁹ which is defined such that $V_1 = +V_{bias}/2$ and $V_2 = -V_{bias}/2$, where $V_{bias} = V_1 - V_2$ is the voltage across the dot in the current path that is consistent with a bias current I . The measured voltage V in the experiments corresponds to the quantity $V = V_3 - V_4$, and the non-local resistance is then

$$R_{nl} = \frac{V_3 - V_4}{I}. \quad (2)$$

We obtain the mean and root-mean-square (rms) of the R_{nl} by generating a set of random scattering matrices with the kicked rotator^{23,24}. The kicked rotator gives a stroboscopic description of the dynamics in the quantum dot, which is a good approximation of the real dynamics for time scales larger than the time of flight across the dot. The particular implementation we used is described in detail in Ref. 40. In a certain parameter range, this model gives results which are equivalent to random matrix theory³. In our simulations we use parameters in this range, the details of which can be found in Ref. 40.

Figure 6 presents the results from these numerical simulations. We focus on analysis of the fluctuations in R_{nl} , since the mean values of R_{nl} simply always gave zero, in agreement with the experimental results²¹. Figure 6a shows the dependence of the fluctuations in R_{nl} on the total number of open channels in the voltage probes $N_{V_+} + N_{V_-}$, for systems with time-reversal symmetry ($\beta = 1$) and broken time-reversal symmetry ($\beta = 2$). The results

in Fig. 6b show that the fluctuations in R_{nl} have (besides a strong dependence on $N_{V_+} + N_{V_-}$ as in Fig. 6a) a weak dependence on the difference $N_{V_+} - N_{V_-}$ (presented only for the case $\beta = 2$). This is not further studied in detail, and the results in Fig. 6a present values that are averaged over all the possible combinations $N_{V_+} - N_{V_-}$, as in the analysis of the experimental results.

Qualitatively, the theoretical results of Fig. 6a agree very well with the experimental results of Fig. 5. However, while the model system gives non-local resistance R_{nl} values that fluctuate with an rms value of a few k Ω , the experimental values ($\beta = 2$) are only of order 200 Ω . The numerical and experimental values differ by a factor of about 20, as illustrated by the fit in Fig. 5: Fitting the theoretical data points of Fig. 6 on the experimental values, using a simple pre-factor that scales the theoretical values as fitting parameter, gives $0.05 \approx \frac{1}{20}$ for this pre-factor.

The discrepancy between the numerical and the experimental results is most likely due to the presence of a dephasing mechanism for electrons inside the quantum dot (and possibly due to the finite temperature of 130 mK in the experiments). Moreover, such dephasing is consistent with the simple scaling that was needed to obtain agreement between theory and experiment. Theory for two-terminal quantum dots gives that the influence of dephasing on the amplitude of conductance fluctuations is that it scales the amplitude down by a factor $(1 + \tau_d/\tau_\phi)$, where τ_d is the mean dwell time in the dot and τ_ϕ is the dephasing time^{36,41}. Assuming a similar approach for our system, and that the reduced amplitude of the fluctuations in our experiment is mainly due to dephasing, gives $(1 + \tau_d/\tau_\phi) \approx 20$ for our system.

VI. CONCLUSIONS

We investigated quantum fluctuations in electron transport with a ballistic, chaotic quantum dot that was

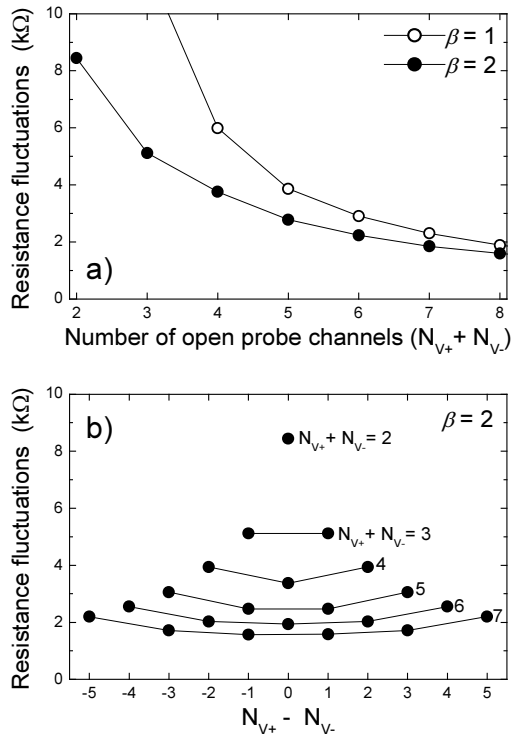


FIG. 6: a) Theoretical rms values of fluctuations in the non-local resistance (ΔR_{nl}), as a function of the total number open of channels in the voltage probes $N_{V+} + N_{V-}$. The two curves present results for a system with ($\beta = 1$) and without ($\beta = 2$) time-reversal symmetry. The QPCs for the current path were assumed to have a conductance of $2e^2/h$. The data is obtained from a Landauer-Büttiker description of the quantum dot system and numerical simulations based on random matrix theory. b) Theoretical rms values of fluctuations in R_{nl} , as a function of the difference in number open of channels in the two voltage probes, $N_{V+} - N_{V-}$, at fixed values of $N_{V+} + N_{V-}$, that have been averaged over all possible combinations of $N_{V+} - N_{V-}$.

strongly coupled to four reservoirs via quantum point contacts. The four-terminal geometry allowed for studying fluctuations in the non-local resistance. We used the dependence of the non-local resistance fluctuations on bias voltage, gate voltage and magnetic field to show that these are the equivalent of universal conductance fluctuations in two-terminal systems, and we showed that with a four-terminal system these fluctuations can be studied without being hindered by Coulomb-blockade and weak-localization effects. Furthermore, the four-terminal geometry was used to demonstrate directly that the amplitude of fluctuations in electron transport is reduced when the coupling between a quantum dot system and voltage probes is enhanced. Here, we obtain good qualitative agreement with a model based on Landauer-Büttiker formalism and random matrix theory, but a quantitative evaluation indicates that there is an intrinsic orbital dephasing mechanism that reduces the amplitude of the non-local resistance fluctuations. Our results are of importance for further work with four-terminal quantum dots on dephasing and electron-spin dynamics in such systems, where the electron-transport signals of interest will always have fluctuations of the type that is reported here.

Acknowledgments

We thank Dominik Zumbühl and Carlo Beenakker for discussions, and the Dutch Foundation for Fundamental Research on Matter (FOM) for financial support. JHB acknowledges support by the European Community's Marie Curie Research Training Network under contract MRTN-CT-2003-504574, Fundamentals of Nanoelectronics.

- ¹ B. L. Al'tshuler and P. A. Lee, *Physics Today*, Issue of December 1988, p. 36.
- ² C. W. J. Beenakker and H. van Houten, *Sol. State Phys.* **44**, 1 (1991).
- ³ C. W. J. Beenakker, *Rev. Mod. Phys.* **69**, 731 (1997).
- ⁴ Y. Imry, *Introduction to Mesoscopic Physics* (Oxford University Press, Oxford, 2002).
- ⁵ A. G. Huibers, M. Switkes, and C. M. Marcus, *Phys. Rev. Lett.* **81**, 200 (1998).
- ⁶ A. G. Huibers *et al.*, *Phys. Rev. Lett.* **81**, 1917 (1998).
- ⁷ E. R. P. Alves and C. H. Lewenkopf, *Phys. Rev. Lett.* **88**, 256805 (2002).
- ⁸ D. M. Zumbühl *et al.*, *Phys. Rev. B* **72**, 081305 (2005).
- ⁹ M. Büttiker, *Phys. Rev. Lett.* **57**, 1761 (1986).
- ¹⁰ A. Benoit, C. P. Umbach, R. B. Laibowitz, and R. A. Webb, *Phys. Rev. Lett.* **58**, 2343 (1987).
- ¹¹ W. J. Skocpol *et al.*, *Phys. Rev. Lett.* **58**, 2347 (1987).
- ¹² H. Haucke, S. Washburn, A. D. Benoit, C. P. Umbach, and R. A. Webb, *Phys. Rev. B*, **41**, 12454 (1990).
- ¹³ M. Büttiker, *Phys. Rev. B*, **40**, 3409 (1989).
- ¹⁴ H. U. Baranger and P. A. Mello, *Phys. Rev. Lett.* **73**, 142 (1994).
- ¹⁵ R. M. Potok, J. A. Folk, C. M. Marcus, and V. Umansky, *Phys. Rev. Lett.* **89**, 266602 (2002).
- ¹⁶ A. Venkatesan, S. Frolov, J. Folk, and W. Wegscheider, 2007 March Meeting Bulletin of the American Physical Society (unpublished), Abstract H12.00012.
- ¹⁷ F. J. Jedema, A. T. Filip, and B.J. van Wees, *Nature* **410**, 345 (2001).
- ¹⁸ J. A. Folk, R. M. Potok, C. M. Marcus, and V. Umansky, *Science* **299**, 679 (2003).
- ¹⁹ D. M. Zumbühl *et al.*, 2001 March Meeting Bulletin of the American Physical Society (unpublished), Abstract C25.006.

- ²⁰ C. W. J. Beenakker, Phys. Rev. B **73**, 201304 (2006).
- ²¹ J. H. Bardarson, I. Adagideli, and P. Jacquod, Phys. Rev. Lett. **98**, 196601 (2007).
- ²² R. Landauer, IBM J. Res. Dev. **1**, 223 (1957).
- ²³ F. M. Izrailev, Phys. Rep. **196**, 299 (1990).
- ²⁴ Y.V. Fyodorov and H.-J. Sommers, JETP Lett. **72**, 422 (2000).
- ²⁵ B. J van Wees *et al.*, Phys. Rev. Lett. **60**, 848 (1988).
- ²⁶ D. Wharam *et al.*, J. Phys. C: Solid State Phys. **21**, L209 (1988).
- ²⁷ P. Debray, J.-L. Pichard, J. Vicente, and P. N. Tung, Phys. Rev. Lett. **63**, 2264 (1989).
- ²⁸ J. A. Folk *et al.*, Phys. Rev. Lett. **86**, 2102 (2001).
- ²⁹ D. M. Zumbühl *et al.*, Phys. Rev. B **69**, 121305 (2004).
- ³⁰ C. M. Marcus *et al.*, Chaos Solitons Fractals **8**, 1261 (1997); cond-mat/9703038.
- ³¹ A. G. Huibers *et al.*, Phys. Rev. Lett. **83**, 5090 (1999).
- ³² C. W. J. Beenakker and H. van Houten, Phys. Rev. B **37**, 6544 (1988).
- ³³ H. van Houten *et al.*, Phys. Rev. B **39**, 8556 (1989).
- ³⁴ K. Kobayashi, H. Aikawa, S. Katsumoto, and Y. Iye, J. Phys. Soc. Japan, **71**, 2094 (2002).
- ³⁵ G. Seelig, S. Pilgram, A.N. Jordan, and M. Büttiker, Phys. Rev. B **68**, 161310 (2003).
- ³⁶ P. W. Brouwer and C. W. J. Beenakker, Phys. Rev. B **51**, 7739 (1995).
- ³⁷ P. W. Brouwer and C. W. J. Beenakker, Phys. Rev. B **55**, 4695 (1997).
- ³⁸ Analysis of the error bars is in particular relevant for low values of $N_{V+} + N_{V-}$, for which we could only obtain a few independent fluctuations. We used that we had the largest amount of data for traces with $N_{V+} + N_{V-} = 7$. Here we had sufficient data to estimate $\Delta R_{nl} = 126 \pm 56 \Omega$. For traces with lower $N_{V+} + N_{V-}$, we used that the number of independent fluctuations n_f along a trace with constant $N_{V+} + N_{V-}$ is simply proportional to $N_{V+} + N_{V-}$ for data sets as in Fig. 2, since it is proportional to the trace length through the data set. We assume a gaussian distribution for the fluctuations. Then, we used that for a finite number n_f of independent fluctuations, the error bar for $\langle R_{nl} \rangle$ depends on n_f as $1/\sqrt{n_f}$, and for ΔR_{nl} (on the same scale) as $1/\sqrt{2n_f}$.
- ³⁹ Note that this definition for ground differs from the grounding used in the experiment. However, since in our experiments the values of the gate voltages were much larger than the values of V_{bias} , our theoretical model is a valid description of the experiment.
- ⁴⁰ J. H. Bardarson, J. Tworzydło, and C. W. J. Beenakker, Phys. Rev. B **72**, 235305 (2005).
- ⁴¹ H. U. Baranger and P. A. Mello, Phys. Rev. B **51**, 4703 (1995).